scientific reports

Check for updates

OPEN

Transcriptional coupling and repair of 8-OxoG activate a RecA-dependent checkpoint that controls the onset of sporulation in *Bacillus subtilis*

Valeria P. Suárez[1,4], Lissett E. Martínez[1,4], Hilda C. Leyva-Sánchez[1], Luz I. Valenzuela-García[1], Reyna Lara-Martínez[3], Luis F. Jiménez-García[3], Norma Ramírez-Ramírez[1], Armando Obregon-Herrera[1], Mayra Cuéllar-Cruz[1], Eduardo A. Robleto[2] & Mario Pedraza-Reyes[1]✉

During sporulation *Bacillus subtilis* Mfd couples transcription to nucleotide excision repair (NER) to eliminate DNA distorting lesions. Here, we report a significant decline in sporulation following Mfd disruption, which was manifested in the absence of external DNA-damage suggesting that spontaneous lesions activate the function of Mfd for an efficient sporogenesis. Accordingly, a dramatic decline in sporulation efficiency took place in a *B. subtilis* strain lacking Mfd and the repair/prevention guanine oxidized (GO) system (hereafter, the ΔGO system), composed by YtkD, MutM and MutY. Furthermore, the simultaneous absence of Mfd and the GO system, (i) sensitized sporulating cells to H_2O_2, and (ii) elicited spontaneous and oxygen radical-induced rifampin-resistance (Rif^r) mutagenesis. Epifluorescence (EF), confocal and transmission electron (TEM) microscopy analyses, showed a decreased ability of ΔGO Δ*mfd* strain to sporulate and to develop the typical morphologies of sporulating cells. Remarkably, disruption of *sda*, *sirA* and *disA* partially, restored the sporulation efficiency of the strain deficient for Mfd and the ΔGO system; complete restoration occurred in the $RecA^-$ background. Overall, our results unveil a novel Mfd mechanism of transcription-coupled-repair (TCR) elicited by 8-OxoG which converges in the activation of a RecA-dependent checkpoint event that control the onset of sporulation in *B. subtilis*.

When conditions are no longer appropriate for growth, a subpopulation of stationary-phase *B. subtilis* cells triggers a developmental pathway leading to the synthesis of highly resistant and differentiated cells, termed spores[1,2]. During the initial stages of this developmental process, the sporulating cells experience an asymmetric cell division that generates two compartments of different size, the mother cell (larger compartment) and the forespore (smaller compartment)[3]. During the early sporulation stages the chromosome exhibits a final round of replication to ensure the existence of two chromosomal copies during the asymmetric division. Upon establishment of the sporulation septum one of these chromosomal copies segregates to the forespore compartment[1,3]. From this step forward, sporogenesis is orchestrated by a spatio-temporal program of gene expression taking place in both cross talking compartments[1,3–5]. It has been proposed that the damages inflicted to the sporangia's chromosomes must be immediately corrected to prevent deficiencies in this developmental program and insure a proper sporulation process[6–8]. Previous observations have revealed that sporulating cells deploy repair and tolerance mechanisms to safeguard the integrity of the sporangia's chromosomes[9–13]. Accordingly, in sporangia, helix-distorting DNA lesions inflicted by ultraviolet C light and mitomycin C are mainly processed by the transcriptional coupling repair (TCR) factor Mfd and the nucleotide excision repair pathway (NER)[13,14]. Furthermore,

[1]Division of Natural and Exact Sciences, Department of Biology, University of Guanajuato, Guanajuato, Mexico. [2]School of Life Sciences, University of Nevada, Las Vegas, NV, USA. [3]Department of Cell Biology, Faculty of Sciences, National Autonomous University of Mexico (UNAM), Circuito Exterior, Ciudad Universitaria, Cd. Mx., Coyoacán, 04510 Mexico City, Mexico. [4]These authors contributed equally: Valeria P. Suárez and Lissett E. Martínez. ✉email: pedrama@ugto.mx

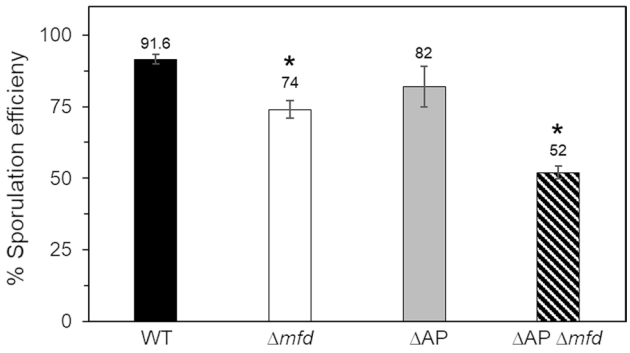

Figure 1. Sporulation efficiency of strain 168 derivatives. The strains were induced to sporulate in DSM for 24 h at 37 °C and assessed for sporulation efficiency by the heat-killing method. Asterisks indicate statistically significant differences between strains as determined by one-way analysis of variance (ANOVA) followed by a Tukey's post-hoc test; $P < 0.05$. Values are expressed as mean values ± standard deviation of at least three independent experiments.

a recent report revealed that the SOS response is active during sporulation and that RecA, is required to counteract genetic lesions inflicted by physical and alkylating factors[9]. However, two additional sporulation roles have been attributed to RecA, firstly as a factor that regulates the levels of phosphorylated Spo0A during the onset of sporulation, and secondly blocking replication and vegetative growth in further stages of this developmental pathway[15–17]. As noted above, Mfd and the NER system counteract the cytotoxic and genotoxic effects promoted by physical and chemical factors that promote bulky DNA lesions[13,18–20]. However, in the absence of external DNA damaging factors, the sole absence of Mfd affected sporulation in *B. subtilis*[13], suggesting that spontaneous DNA lesions in actively transcribed genes require Mfd for a proper sporogenesis. In support of this concept, here we report that disabling of the repair/prevention guanine oxidized (GO system) in a Mfd-deficient genetic background induced a marked decrease in *B. subtilis* sporulation. Results from TEM and confocal microscopies demonstrated the sporulation defect, including, the incapability of the Δ*mfd* ΔGO strain to generate typical sporangia and mature spores. Furthermore, in reference to WT sporulating cells, the ΔGO Δ*mfd* mutant was severely affected by the ROS-promoter agent H_2O_2 and exacerbated its spontaneous and oxygen radical-induced mutagenesis. Interestingly, disruption of *recA*, *sda, disA* or *sirA* suppressed the sporulation deffect exhibited by the YtkD/MutM/MutY/Mfd-deficient strain. Overall our results support the notion that transcriptional coupling of 8-OxoG repair activates checkpoint events dependent on RecA, Sda, SirA and DisA with a direct impact on the onset and progression of *B. subtilis* sporulation.

Results

Mfd and the GO system are required for an efficient sporulation process in *B. subtilis*. A previous report revealed that inactivation of *mfd* affected the sporulation process of *B. subtilis*, even in the absence of external genotoxic factors[13]. To explore whether spontaneous DNA lesions elicited by ROS are involved in this sporulation defect, the AP-endonucleases Nfo, ExoA, Nth or the full GO system[21] were disabled in a *B. subtilis mfd* knockout, and the resulting strains were tested for sporulation efficiency. While no obvious effects were observed in the ΔAP or ΔGO strains; the absence of Mfd resulted in a significant decline in sporulation in comparison with the WT parental strain (Fig. 1). Strikingly, while *mfd* disruption in the ΔAP strain decreased ~ 40% the sporulation efficiency (Fig. 1); the developmental sporulation process was almost completely abolished following disruption of Mfd in the ΔGO strain (Fig. 2A).

Confocal phase-contrast microscopy analysis of cell samples collected during the stage t_9 of the sporulation process corroborated that while the WT, Δ*mfd* and ΔGO strains generated typical sporangia with mature refringent spores, in this stage, the Δ*mfd* ΔGO strain was incapable of generating cells with a typical sporulating phenotype (Fig. 2B). Altogether, these results strongly suggest that AP sites and 8-OxoG lesions that compromise sporulation require a functional Mfd protein.

The GO system together with Mfd contributes to an efficient *B. subtilis* sporulation process. The strong sporulation defect detected in the Δ*mfd* ΔGO strain was of interest and further analyzed. The simultaneous action of the three components of the GO system counteract the mutagenic and cytotoxic effects of 8-OxoG; however, they accomplish this task through different mechanisms. Whereas MutM specifically hydrolyzes 8-OxoG from DNA, MutY catalyzes the elimination of adenine incorrectly paired with oxidized guanine[22–24]. In contrast, following hydrolysis of 8-Oxo-dGTP, the nucleotide diphosphohydrolase YtkD, avoids the incorporation of 8-OxoG to replicating DNA[25,26]. Therefore, we disabled one or two genes encoding functions of the GO system in the Mfd-deficient strain to better measure their independent and combined contributions to the sporulation process of this strain. Our results revealed similar sporulation efficiencies among the *mfd* strain and its derived strains which carried single disruptions on *mutM*, *mutY* or *ytkD* (Figs. 2, 3). However, a significant decline in sporulation was observed upon disruption of two gene encoding components of the GO system in the Δ*mfd* strains. The simultaneous disruption of *mutM*/*mutY*, *mutY*/*ytkD* or *mutM*/*ytkD* decreased the sporulation efficiency of the strain lacking Mfd between 40 and 50% (Figs. 2, 3). Overall, these results and

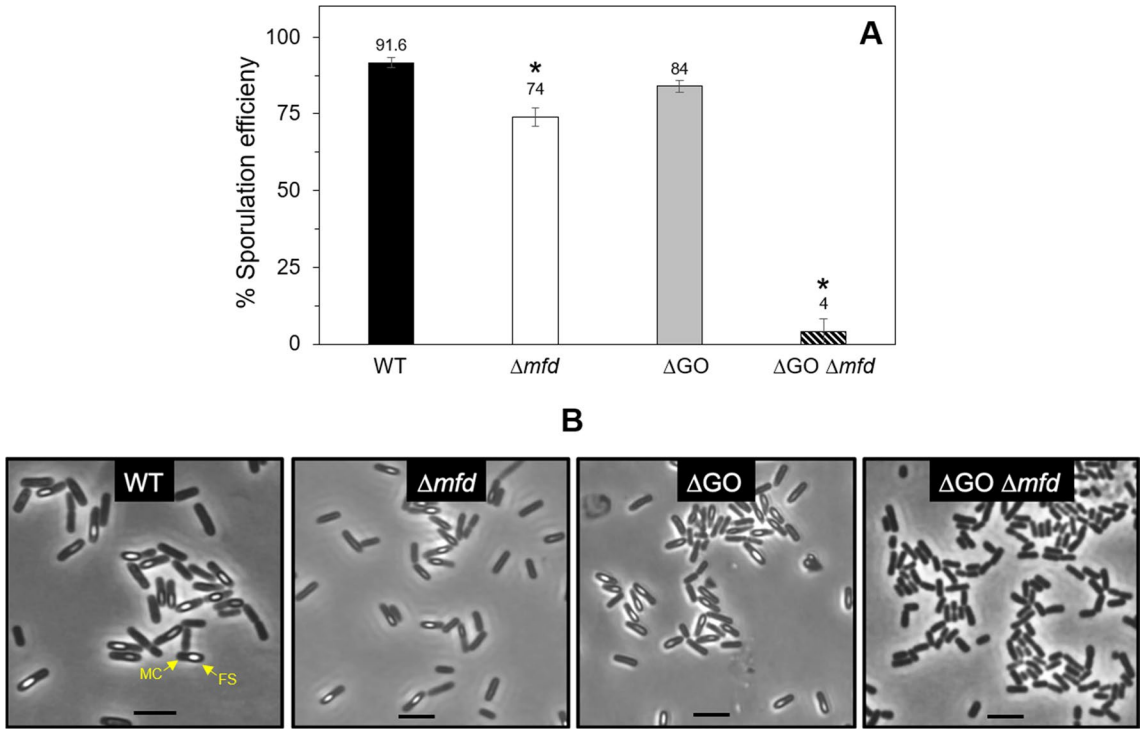

Figure 2. (**A**) Sporulation efficiency of strain 168 derivatives. The strains were induced to sporulate in DSM for 24 h at 37 °C and assessed for sporulation efficiency by the heat-killing method. Asterisks indicate statistically significant differences between strains as determined by one-way analysis of variance (ANOVA) followed by a Tukey's post-hoc test; $P < 0.05$. Values are expressed as mean values ± standard deviation of at least three independent experiments. (**B**) Strains indicated were induced to sporulate at 37 °C, and 9 h after t_0, cell samples were collected and analyzed by confocal microscopy as described in "Materials and methods" section. MC and FS, mother cell and forespore compartments. The scale bar is 2 µm.

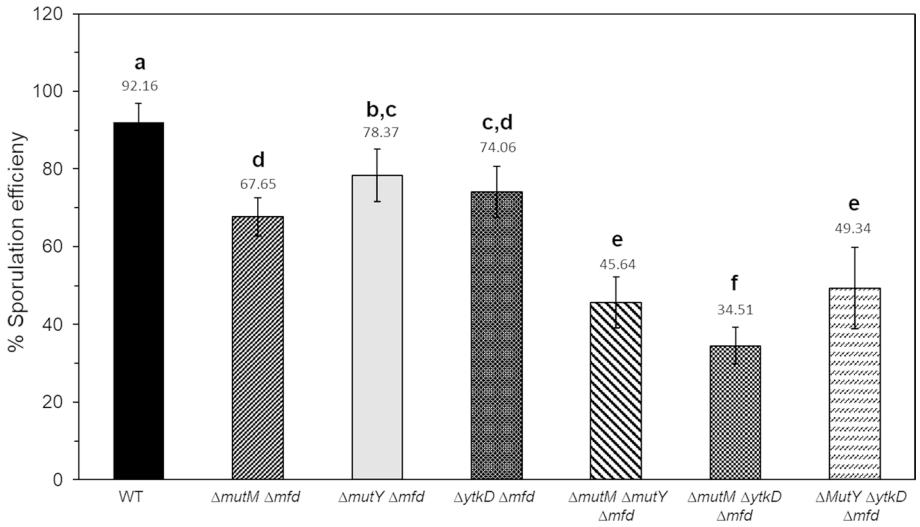

Figure 3. Sporulation efficiency of strain 168 derivatives. The strains were induced to sporulate in DSM for 24 h at 37 °C and assessed for sporulation efficiency by the heat-killing method. Letters a, b, c and d, indicate significant differences between strains as determined by one-way analysis of variance (ANOVA) followed by a Tukey's post-hoc test; $P < 0.05$. Values are expressed as mean values ± standard deviation of at least three independent experiments.

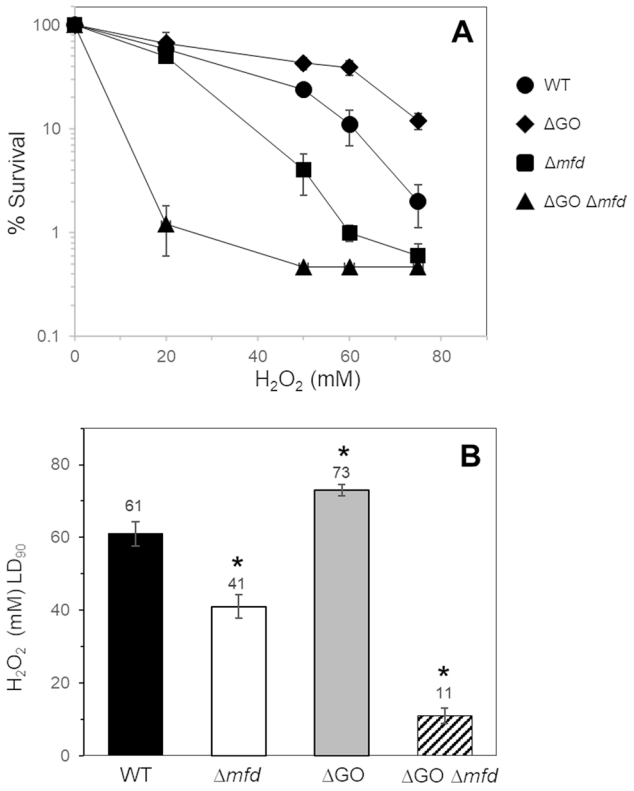

Figure 4. (**A**) Resistance to H_2O_2 of strain 168 derivatives during sporulation. Sporulating cells of strains *B. subtilis* wild type (WT; filled circle), ΔGO (filled diamond), Δ*mfd* (filled square) and ΔGO Δ*mfd* (filled triangle) were treated with increasing doses of H_2O_2 at 4.5 h after the onset of sporulation, and cell survival was determined as described in Materials and Methods. The LD_{90} values (**B**) were calculated for each strain from the dose–response graphs (**A**). Data are expressed as the average ± SD of at least three independent experiments. Asterisks indicate statistically significant differences between strains as determined by one-way analysis of variance (ANOVA) followed by a Tukey's tests; $P < 0.05$.

those shown in Fig. 2, indicate that disruption of the three components of the GO system is necessary to induce a marked decrease in the sporogenesis of the Mfd-deficient strain.

The GO system and Mfd confers protection to sporulating cells from ROS-promoted DNA damage and mutagenesis. The TCR factor Mfd and the prevention/repair GO system are required for *B. subtilis* sporogenesis (Fig. 1). Therefore, we determined the effects of single and combined deficiencies of both functions on the protection of sporulating cells from the noxious effects of the oxidizing agent H_2O_2. Results revealed that compared with the WT strain, disabling of *mfd* sensitized sporulating cells to H_2O_2; in contrast, the ΔGO cells exhibited a higher resistance to the oxidizing agent (Fig. 4A). Notably, the Δ*mfd* ΔGO strain exhibited a significantly higher susceptibility to H_2O_2 than the WT and Δ*mfd* strains (Fig. 4A); in summary, the WT, Δ*mfd*, ΔGO and ΔGO Δ*mfd* strains exhibited lethal dose 90 s (LD_{90s}) of, 61 ± 4, 41 ± 3.5, 73 ± 2.5 and 11 ± 2, respectively (Fig. 4B). In nutritionally stressed non-replicating *B. subtilis* cells, the GO system prevented stress-associated mutagenesis while Mfd played a promutagenic role[21,27–29]. In the present report, we found that in sporulating cells, the absence of Mfd or the GO system induced a significant increase in the spontaneous and H_2O_2-promoted mutagenesis in comparison with the WT strain (Fig. 5). Of note, during sporulation, the spontaneous and induced mutagenesis values were significantly higher in the ΔGO Δ*mfd* strain than in the Mfd- or ΔGO-deficient strains (Fig. 5). Altogether, these results suggest that Mfd and the GO system protect sporulating cells from ROS-promoted DNA lesions that compromise sporulation.

Cytological analysis of strain *B. subtilis* WT and ΔGO Δ*mfd* by epifluorescence and TE-microscopy. As noted above, the simultaneous absence of a complete GO system and Mfd markedly decreased *B. subtilis* sporulation. Importantly, exponentially growing cells of this strain as well as those from strains with a disabled GO system or Mfd did exhibit similar doubling times and cellular morphologies as those detected in the wild-type strain by confocal microscopy (Fig. S1). In *B. subtilis* the sporulation process, which takes place during the stationary phase of growth, is defined by specific and well differentiated morphological steps (arbitrarily termed stages t_0–t_9)[1,3]. The first unequivocal manifestation of sporulation in *B. subtilis*, which occurs during stage t_2, is characterized by the synthesis of an asymmetric cell division septum and the formation of a two-compartment asymmetric sporangium[3,30,31]. A subsequent temporal pattern of gene expression in each

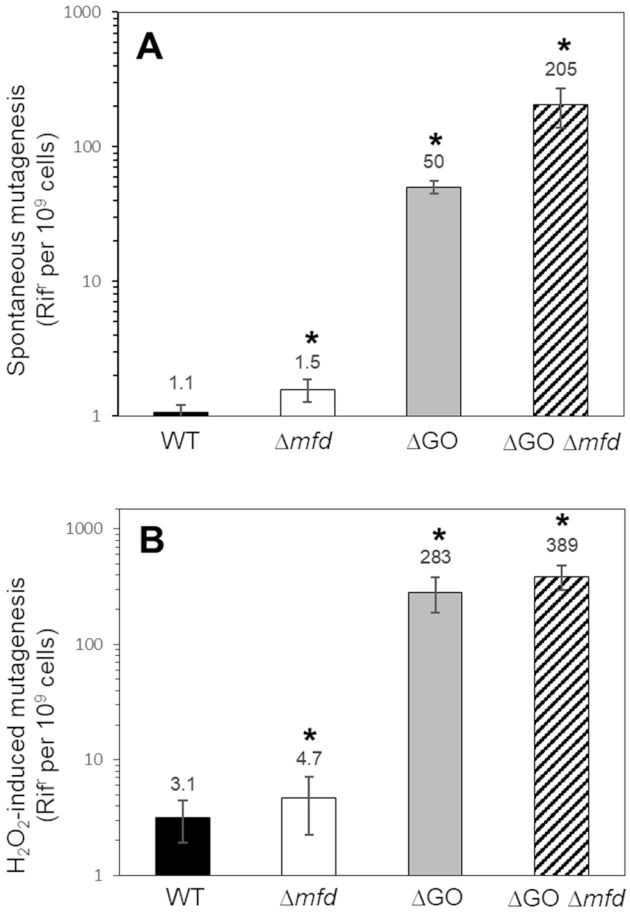

Figure 5. Frequencies of mutation to Rif^r. Cells of *B. subtilis* wild type (WT; black bars), ΔGO (gray bars), Δ*mfd* (white bars) and ΔGO Δ*mfd* (hatched bars) strains, were sporulated in liquid DSM and left untreated (**A**) or treated (**B**) with the LD_{50} for each strain of H_2O_2 (**B**) at 4.5 h after the onset of sporulation. The levels of Rif^r cells with (**B**) or without (**A**) treatment exposure were determined. Each bar represents the the average ± SD of at least three independent experiments. Asterisks indicate statistically significant differences between strains as determined by U Mann–Whitney test; $P < 0.05$.

compartment drives the synthesis and maturation of an endospore[1,31–33]. Therefore, we examined ΔGO Δ*mfd* cells during sporulation for developmental morphological defects using epifluorescence (EF) and transmission electron microscopies (TEM). To this end, we collected samples of cultures at different stages during sporulation and stained their DNA and membrane with DAPI and FM4-64 dyes, respectively. In comparison to cells of the wild-type strain, the EF microscopic analysis revealed a number of morphological defects in the ΔGO Δ*mfd* mutant that began to manifest at the sporulation stage t_2; firstly, the absence of cells with asymmetric septa (stage t_2); secondly, the inability to progress into sporangia with well-defined mother cell and forespore compartments (t_5), and, finally, the failure to generate mature endospores (t_9) (Fig. 6).

The sporulation defect of the Mfd/GO-deficient strain, appeared to develop from the initial stages of sporulation and was analyzed in depth by TE microscopy. To this end, WT and ΔGO Δ*mfd* cells collected during sporulation stages t_0, t_3, t_5 and t_9 were fixed with glutaraldehyde and processed for TEM as described in Materials and Methods. During stage t_0, both, the WT and the strain deficient for GO and Mfd, presented typical vegetative cellular morphologies; however, cells from the latter strain exhibited anomalous thick division septa (Fig. 7). Remarkably, the strain lacking the GO system and *mfd* did not experience the morphological events of asymmetrical cell division and forespore engulfment occurring during stages t_3 and t_5 in the wild type sporulating cells (Fig. 7). Indeed, during stages t_3 and t_5, the mutant generated dividing cells with aberrant morphologies and failed, during stage t_9, to generate the typical sporangia with endospores and free spores as observed in the wild type strain (Fig. 7). In summary, these results not only attest for the failure in sporogenesis of the ΔGO Δ*mfd* strain, but also suggest that such phenotype was the product of defects that began at the initial stages of this developmental process.

RecA, Sda, DisA and SirA regulate the sporulation defect of *B. subtilis* cells lacking a functional GO system and transcription-coupling repair. The cellular defects exhibited by the ΔGO Δ*mfd* strain prompted us to investigate the existence of a possible checkpoint event blocking the onset of sporulation in this mutagenic, repair-deficient strain. Because the mutant failed to produce cells with typical morphologies in stage

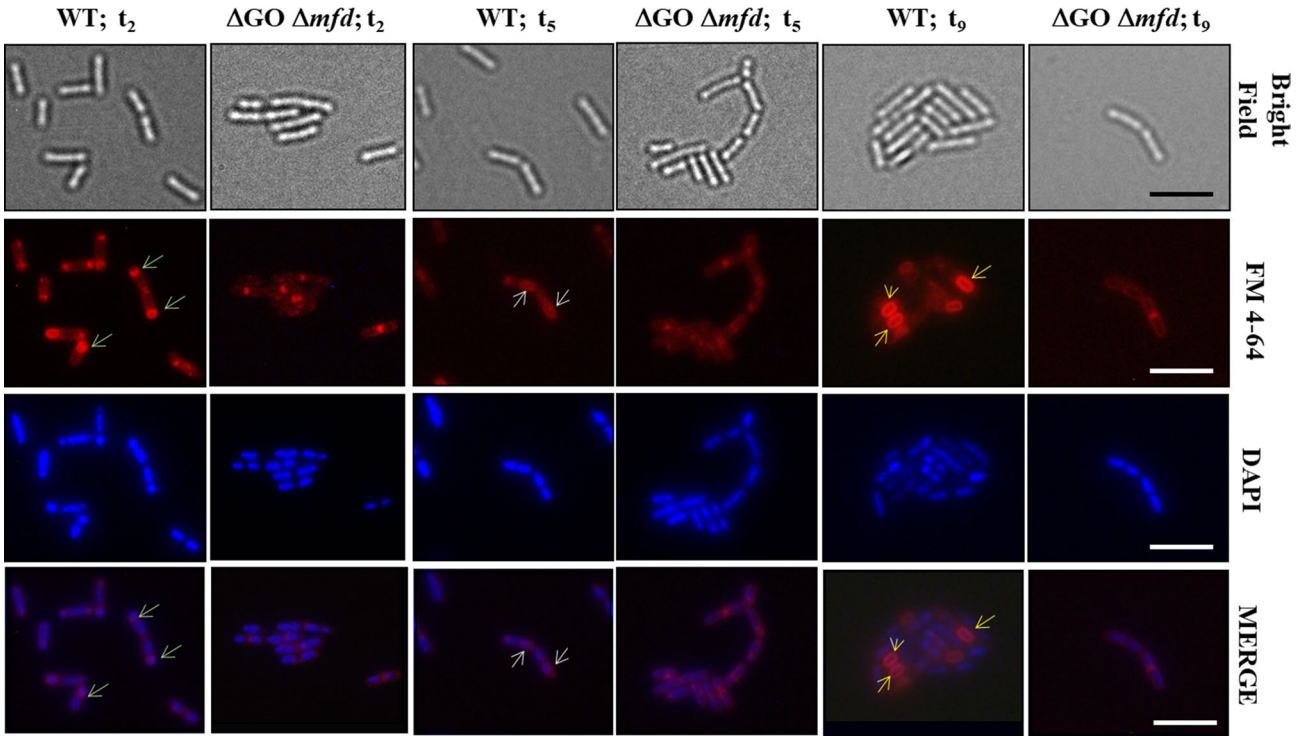

Figure 6. Epifluorescence microscopic analysis of sporulation stages of *B. subtilis* strains with a wild type (WT) or Δ*mfd*/ΔGO genotype. The strains indicated were induced to sporulate in DSM. At the indicated stages (t_2, t_5 and t_9), cells were collected, fixed and analyzed by bright- field (BF) and fluorescence (DAPI and FM4-64 staining) microscopy as described in "Materials and methods" section. Overlain images of DAPI and FM4-64 at each time point are depicted as MERGE. Yellow arrowheads show the proper development of the forespore in the WT strain during the stages analyzed. The scale bar is 5 μm and all images are at the same magnification.

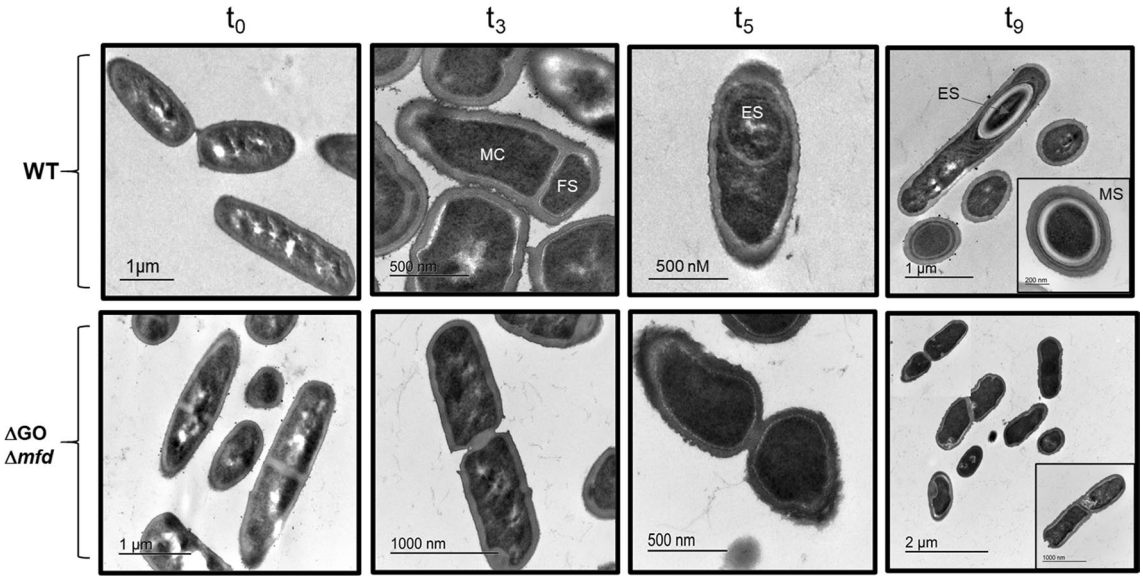

Figure 7. Transmission electron microscopy of sporulation stages of *B. subtilis* strains with a wild type (WT) or Δ*mfd* ΔGO genotype. The strains indicated were induced to sporulate in DSM. At the stages indicated (t_0, t_3, t_5 and t_9), cells were collected, fixed and analyzed by TEM as described in "Materials and methods" section. Red arrows indicate: *MC* mother cell, *FS* forespore, *ES* endospore, *MS* mature spore. Insets in stage t_9 show: Upper panel, section of a mature spore; Lower pannel, section of an aberrant non-sporulated, divided cell. Scale bars as indicated in the panels.

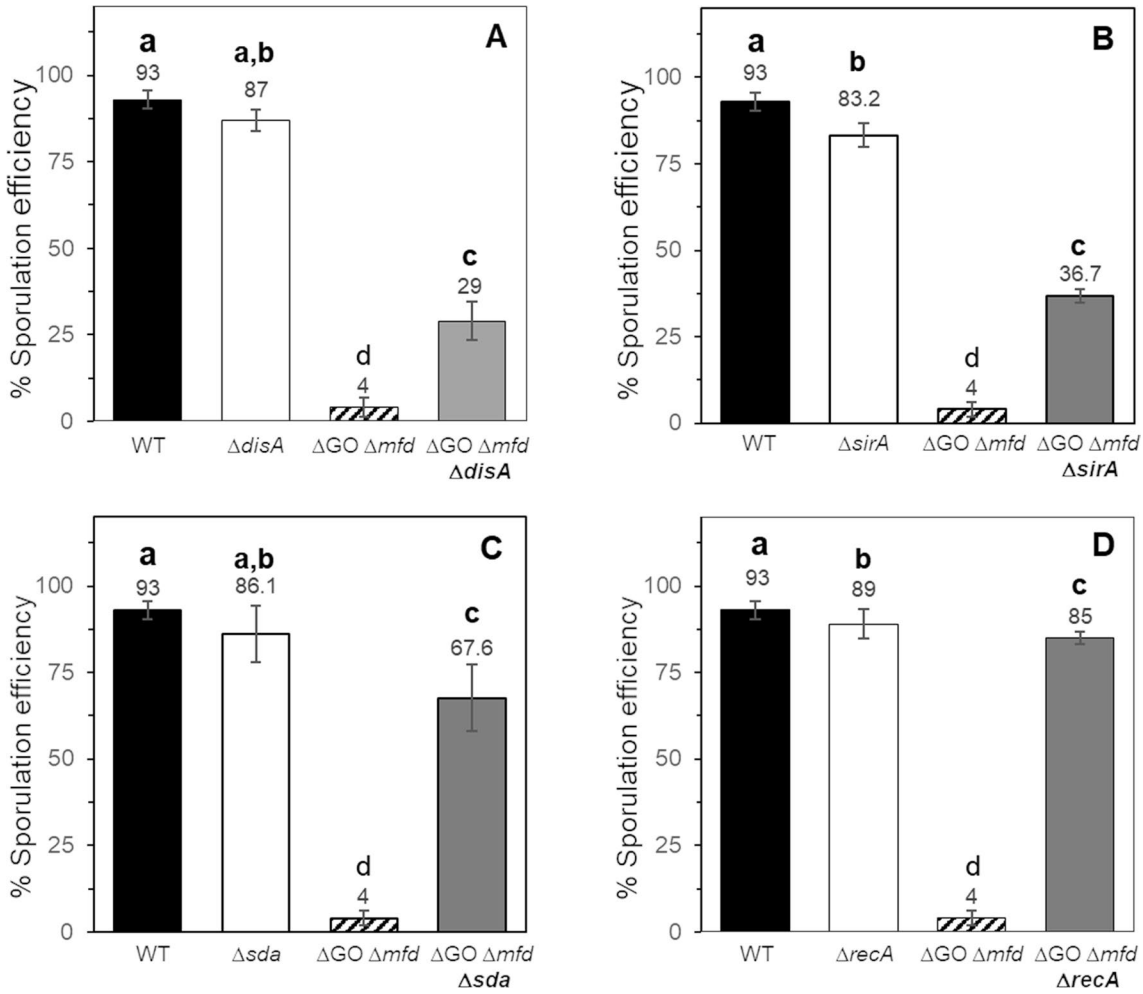

Figure 8. Analysis of suppressors of the sporulation defect of the strain *B. subtilis* Δ*mfd* ΔGO. The strains indicated were induced to sporulate in DSM for 24 h at 37 °C and assessed for sporulation efficiency by the heat-killing method. Letters a, b, c and d, indicate statistically significant differences between strains as determined by one-way analysis of variance (ANOVA) followed by a Tukey's post-hoc test; $P < 0.05$. Values are expressed as mean values ± standard deviation of at at least three independent experiments.

t_2 sporangium, we first considered DisA. This octameric protein delays the segregation of one chromosomal copy to the sporangia's forespore compartment when DNA damage is encountered during stages t_2–t_3[7,34]. The results of our genetic analysis revealed that disruption of *disA* significantly, but not completely, improved the sporulation efficiency of the quadruple knockout *ytkD mutM mutY mfd* strain (Fig. 8A). Based on these results we speculated that additional factor(s) must be involved in promoting the developmental defects observed in this mutant strain.

TEM analysis of the ΔGO Δ*mfd* strain showed a sporulation defect in this strain from the onset of sporulation (Fig. 7). Therefore, our analysis to identify suppressors of the sporulation defect exhibited by the ΔGO Δ*mfd* strain was extended to SirA (Sporulation inhibitor of Replication), a checkpoint protein that ensures the existence of a single chromosomal copy in each of the cell compartments of *B. subtilis* sporangia[8,35]. Disruption of *sirA* resulted in a partial restoration of the sporulation efficiency of the ΔGO Δ*mfd* strain following disruption of *sirA* (Fig. 8B). Therefore, it is possible to speculate that the exacerbated DNA damage occurring in the ΔGO Δ*mfd* strain activates SirA- and DisA-controlled checkpoint functions[7,8,34,35]. It has been shown that sporulation is inhibited if cells committed to this developmental process sense genetic alterations or conditions that interfere with DNA replication[6,8,16], and that this inhibition is mediated by the multifunctional protein RecA[9,15]. Strikingly, the levels of sporulation efficiency were almost completely reestablished to those exhibited by the wild-type strain following disruption of *recA* in the ΔGO Δ*mfd* strain (Fig. 8D). In response to replicative stress and activation of the SOS-response, stationary phase cells induce the synthesis of SdA, a protein that specifically inhibits KinA's autokinase activity, which results in reduced levels of Spo0A-P[6,36]. Our assays revealed that the genetic disruption of *sda* restored the sporulation efficiency of the strain lacking Mfd and a functional GO system (Fig. 8C). Taken together, these results strongly suggest that the DNA-damage dependent checkpoint proteins RecA, Sda, SirA and DisA, in a hierarchical manner (i.e., RecA > Sda > SirA > DisA) regulate the sporulation defect of a *B. subtilis* strain deficient in transcription coupling repair and prone to accumulate 8-OxoG lesions.

The major effect of RecA and Sda in suppressing the sporulation defect of the ΔGO Δ*mfd* strain prompted us to investigate whether its coding genes are upregulated in this genetic background. To test this notion, *recA-lacZ* and *sda-lacZ* transcriptional fusions were recombined in the *recA* or *sda* loci of the WT and ΔGO Δ*mfd* genetic backgrounds and the levels of β-galactosidase were determined in the resulting strains during the sporulation stage t_0. The levels of β-galactosidase exhibited by the strain carrying the *recA-lacZ* fusion were ~ 3.9 times higher in the GO/Mfd-deficient strain than in the WT strain (i.e., 18.2 ± 0.7 vs 4.7 ± 0.7 Miller units). Furthermore, in the strains harboring the *sda-lacZ* fusion the levels of the reporter *lacZ* gene were ~ 11.9 times higher in the ΔGO Δ*mfd* strain than in the WT strain (i.e., 11.9 ± 1.1 vs 0.9 ± 0.1 Miller units). Altogether, these results strongly suggest that the levels of *recA* and *sda* are upregulated in the strain deficient in Mfd and the prevention/repair GO system.

Discussion

Here, we report that the absence of the TCR factor Mfd, induced a marked decrease in the sporogenesis of a *B. subtilis* strain deficient for the repair/prevention GO system. As revealed by TEM and EF microscopies, this mutant failed to generate typical sporangia and developing mature spores. Also, it was found that RecA, Sda, SirA and DisA, which regulate sporulation checkpoint events, are responsible of the sporulation defects observed in the GO/Mfd-deficient strain.

In addition to its classical role in transcriptional coupling repair[14,19], alternative functions have been attributed to Mfd in *B. subtilis*; namely, in conferring protection against protein oxidation[37], as a regulator of carbon catabolite repression as well as in transcription associated mutagenesis of amino acid starved cells[27,28,38].

Here and a previous report[13] revealed an unexpected role for Mfd in endospore formation; essentially, in the absence of external DNA damaging factors, disruption of *mfd* resulted in a significant decrease in the efficiency of *B. subtilis* to generate spores. This result strongly suggests that spontaneous genetic lesions, other than those that cause major DNA distortions, interfere with the expression of genes that are necessary for an efficient sporogenesis. Two lines of evidence support this notion, firstly, around two hundred genes involved in sporulation were repressed during the stationary phase of growth in a Mfd-deficient strain[39]. Secondly, genetic disabling of BER-encoding genes that process AP sites and the highly mutagenic lesion 8-OxoG exacerbated the sporulation defect of the strain lacking Mfd (Figs. 1, 2). Importantly, disabling of all the components of the GO system resulted in a marked decline in sporogenesis in the strain deficient for TCR suggesting multiple types of genetic damages, including, (i) direct oxidation of guanines in DNA, (ii) accumulation of 8-OxG:A and G:A mispairs, and, (iii) oxidation of deoxy-GTP and GTP pools can directly or indirectly contribute to the sporulation defect observed in the Mfd/GO-deficient strain. Therefore, in addition to its TCR-NER functions[13], here, we demonstrated that, under conditions of sporulation, Mfd together with the GO system, confers protection to *B. subtilis* cells from the cytotoxic and mutagenic effect of the ROS promoter agent H_2O_2. Altogether, these results suggest that when ROS-promoted DNA damage is encountered by stationary-phase cells committed to sporulation, Mfd elicits high-fidelity repair events and prevents mutagenesis. Of note, our sporulation results contrast those observed in non-growing stationary-phase *B. subtilis* starved cells; Mfd promoted mutagenesis genetic diversity that increased the likelihood of scaping growth-limiting conditions[27,28,40].

Several lines of research have shown that DNA replication is intimately coordinated with the initiation of sporulation in *B. subtilis*; in this interplay, Sda, SirA, DisA and RecA play prominent roles[6–8,41,42]. Accordingly, results from ultrastructural, confocal and epifluorescence microscopies showed that the absence of Mfd and the GO system generated aberrant cells that failed to develop typical sporangia and progress to advanced sporulation stages (Figs. 6, 7, S2). Furthermore, our suppressors analysis revealed that disruption of *disA*, *sirA*, *recA* and *sda*, restored to different levels the ability to sporulate of the quadruple *mutM mutY ytkD mfd* strain. Previous results have revealed that transcription of *sirA* is activated at the start of sporulation, under control of the master regulator Spo0A, to inhibit replication to the existence of only two chromosomal copies in cells committed to sporulation[8,33,35]. Inactivation of *sirA* partially relieved the sporulation efficiency in the strain deficient for Mfd and the GO system. Therefore, in addition to interfering with replication, SirA seems to play additional roles in sporulation, as cells of this TCR/repair deficient strain were uncapable of adopting typical morphologies of sporulating cells (Fig. 7). Our results also revealed a partial suppression of the sporulation defect exhibited by the GO/Mfd-deficient strain in a DisA-deficient background. We hypothesize that, during the stage t_2 of sporulation, a subpopulation of cells of the quadruple *mfd mutM mutY ytkD* mutant strain accumulate DNA lesions that elicit a DisA-dependent checkpoint event that aborts the establishment of the two cell type sporangia. In support of this notion, (i) during sporulation, the strain deficient for GO and Mfd exhibited repair deficiencies and increased mutagenesis under conditions of oxidative stress, and, (ii) as evidenced by TEM, this mutant did not establish asymmetrically divided sporangia. In *B. subtilis* proficient for Mfd and the GO system, the RecA-dependent SOS response is active and required to protect sporulating cells from the DNA damaging factors UV-C light and M-C[9]. Our results revealed that the marked decrease in the sporulation efficiency observed in the strain deficient for Mfd and the GO system is regulated by RecA; disruption of its encoding gene restored the sporulation efficiency of this mutant to levels slightly lower levels than those exhibited by the WT strain. Based on these observations, is feasible to speculate that in starved, Mfd/GO-deficient *B. subtilis* cells, the accumulation of 8-OxoGs[29,43] or its repair intermediates generates replication and/or transcription stress and activates the RecA-dependent SOS response. In support of this assertion, as shown in this work, the levels of *recA* and *sda* were found to be upregulated in the ΔGO Δ*mfd* mutant; furthermore, in the Sda^- background; Sda^- cells displayed an increase in sporulation efficiency of the GO/Mfd-deficient strain. Accordingly, it has been shown that in cells committed to sporulation the SOS-induction of *sda* inhibits phosphorylation of Spo0A and the initiation of this developmental pathway[6,36]. On the other hand, accumulation of unphosphorylated Spo0A activates the expression of *sirA*, the inhibitor of the replication initiator protein DnaA[35]. In addition, the DNA-damaging conditions

prevailing in the Δ*mfd* ΔGO genetic background may converge in the generation of recombination intermediates that pause the scanning activity of DisA and interferes with the proper establishment of functional sporangia[7,44].

RecA-dependent mechanisms that regulates the initiation of sporulation in *B. subtilis* has been previously described[17]. However, our results contribute two novel aspects to RecA-dependent regulation of the initiation of sporulation, (i) the ROS promoted lesion 8-OxoG can signal the activation of the function of RecA, and, (ii) Mfd couples the level of 8-OxoGs and transcription/replication stress to the activation of the RecA-dependent pathway to impact in the initiation of sporulation.

Materials and methods

Bacterial strains and growth conditions. The *B. subtilis* strains used in this study were derived from strain 168 and are listed in Table S1. The strains were constructed using standard molecular biology techniques[45]. *B. subtilis* strains were routinely incubated at 37 °C in Lysogeny–Broth (LB)[46] medium or Difco sporulation medium (DSM)[47], with shaking. When required, erythromycin (Ery; 5 μg/ml), chloramphenicol (Cm; 5 μg/ml), neomycin (Neo; 10 μg/ml), tetracycline (Tet; 15 μg/ml), spectinomycin (Spc; 100 μg/ml), or rifampicin (Rif; 10 μg/ml) were added to media. For culture of *E. coli* strains harboring plasmids, 100 μg/ml ampicillin was added to the LB medium. Solid media were obtained by adding bacteriology grade agar (15 g/l) to the liquid media.

Transformation of *B. subtilis* was performed through natural competence[48]. Detailed description of *B. subtilis* strains is presented in Supplementary material.

Strains construction. A gene construct to disrupt *sirA* was generated as follows. A 234-bp DNA fragment extending from nucleotides (nt) 58–291 from the *sirA* open reading frame (ORF) was PCR amplified using chromosomal DNA from *B. subtilis* 168. The oligonucleotide primers used for this reaction were 5′-CGGAATTCGGCCGGGAATCGGTTATGTTTGAG-3′ (forward) and 5′-GCGGATCCCTTCATCATAAACGTCGCGTG-3′ (reverse). Restriction sites (underlined) were included in the primers for cloning the amplified product between the EcoRI-BamHI and cloned into the pMutin4cat vector[49] using the *E. coli* strain DH5α. The resulting plasmid pPERM1791 was used to transform *B. subtilis* 168 and PERM1136 to generate *B. subtilis* strains Δ*sirA* (PERM1796) and Δ*ytkD* Δ*mutM* Δ*mutY* Δ*sirA* (PERM1798). To generate a *B. subtilis* strain deficient for GO, Mfd and SirA, competent cells of the strain PERM1390 (Table S1) were transformed with plasmid pPERM1791 to generate the strain *B. subtilis* PERM1801 (ΔGO Δ*mfd* Δ*sirA*).

The ΔGO Δ*sda* Δ*mfd* mutant in the 168 background was generated by transforming strain PERM1808 (Δ*sda*) with genomic DNA isolated from *B. subtilis* strain PERM1573 (ΔGO) (Table S1), to generate the strain PERM1815 (ΔGO Δ*sda*). Subsequently, the genetic inactivation of *mfd* was achieved by transforming competent cells of *B. subtilis* strain PERM1815 with the plasmid pPERM1538 (Cm^R) (Supplemental Table S1), thus generating the strain *B. subtilis* PERM1818 (ΔGO Δ*sda* Δ*mfd*).

A *B. subtilis* strain deficient for GO, RecA and Mfd was constructed as follows. To disrupt *mfd*, competent cells of *B. subtilis* ΔGO (PERM1136)[26] were independently transformed with plasmid pPERM1291 (Table S1) and chromosomal DNA from strain *B. subtilis* PERM688 (Δ*recA*), generating strains *B. subtilis* ΔGO Δ*mfd* (PERM1390) and ΔGO Δ*recA* (PERM1740), respectively. Subsequently, competent cells of the strain PERM1740, were transformed with the plasmid pPERM1291 (Table S1) leading to disruption of *mfd*; thus, generating strain *B. subtilis* PERM1745 (ΔGO Δ*recA* Δ*mfd*). Disruption of *disA* in the genetic background *B. subtilis* PERM1390, was achieved by transforming competent cells of this strain with plasmid pPERM1372[14], to generate the strain *B. subtilis* PERM1751 (ΔGO Δ*recA* Δ*disA*). The appropriate recombination events into the homologous loci were confirmed by PCR using specific oligonucleotide primers and by antibiotic resistance.

The construction of transcriptional *sda-lacZ* and *sirA-lacZ* fusion was performed with the integrative vector pMutin4-cat[49]. To this end, a 180-bp internal fragment of the *sda* gene was amplified by PCR with Vent DNA polymerase (New England BioLabs) using chromosomal DNA from *B. subtilis* 168. The oligonucleotide primers used for the amplification of *sda* fragment were 5′-GCGAATTCCAACTTTTAAGGAGGTGCC-3′ (forward) and 5′-GCGGATCCTACGGAAATAATATGTCCGAGCGA-3′ (reverse). The *sda* PCR fragment was ligated between the EcoRI and BamHI sites of pMUTIN4-cat. The resulting construct, designated pPERM1790 (*sda*::*lacZ*) was propagated in *E. coli* DH5α cells. Plasmid pPERM1790 was used to transform *B. subtilis* 168 and PERM1390 (ΔGO Δ*mfd*), generating strains *B. subtilis* PERM1797 (*sda-lacZ*) and PERM1802 (ΔGO Δ*mfd sda-lacZ*), respectively (Table S1). To generate a strain carrying a *recA-lacZ* fusion in the WT and ΔGO Δ*mfd* genetic background competent cells of strain *B. subtilis* 168 and PERM1390 (ΔGO Δ*mfd*) were transformed with chromosomal DNA isolated from *B. subtilis* PERM115[13], thus generating the strain *B. subtilis* PERM1824 and PERM1825, respectively (Table S1).

Sporulation assays. To determine sporulation efficiency, strains were assessed for the presence of heat-resistant spores, as previously described[13]. Briefly, cells were grown in liquid Difco Sporulation Medium (DSM) for 24 h at 37 °C with shaking. At this time, the total viable CFU/ml was measured by plating aliquots of serial dilutions in PBS and then the cultures were heated at 80 °C for 20 min; the viability was assessed again to determine the number of spores present in each sample.

β-galactosidase activity assay. *B. subtilis* strains 1797, 1802, 1824 and 1825 (Table S1) were grown and sporulated in liquid DSM at 37 °C. Cells samples (1 ml) were harvested by centrifugation during sporulation stage t_0 and the pellets were washed twice with 50 mM Tris–HCl (pH 7.5) and stored at − 20 °C. Cells were disrupted with lysozyme followed by centrifugation, and the levels of β-galactosidase was determined according to a previously described protocol[50], using *ortho*-nitrophenyl-β-D-galactopyranoside (ONPG) as the substrate, and the β-galactosidase activity was expressed in Miller units[46].

Electron microscopy. For transmission electron microscopy analysis, 10 ml samples of NSM cultures from *B. subtilis* strains WT and PERM1390 (ΔGO Δ*mfd*), collected during sporulation stages (t_0, t_3, t_5, and t_9), were mixed with 10 ml of 4% (W/V) glutaraldehyde in 0.1 M sodium Cacodylate buffer, pH 8.3 (Fixation buffer; FB) and incubated 30 min at room temperature. The cell suspension was centrifuged (3800×*g*) for 10 min at room temperature; after eliminating the supernatant, the cell pellets were resuspended in 5 ml of FB and incubated overnight at 4 °C. Next day, the cell samples were washed 5 times with glutaraldehyde-free FB and resuspended in 25 ml of 0.1% (V/V) OsO_4 in 0.05 M sodium cacodylate buffer, pH 7.5 and incubated 24 h at 4 °C. After pelleting (3800×*g*; 12 min/4 °C), the cells were washed 3 times with 0.1 M sodium Cacodylate buffer, pH 7.5 and three times with MQ water. The cell samples pelleted by centrifugation as indicated above, were resuspended in 1% (W/V) melted agar and the suspension was settled at room temperature until solidifying. The agar blocks were cutted in ~ 2 mm slices, mixed with 3% (V/V) uranyl acetate and stored overnight at 4 °C. After adjusting at room temperature, the agar slices were washed 3 times, for 30 min, with MQ water and stored at 4 °C[51].

Agar embedded cells were then dehydrated through an ethanol series. Next, samples were immersed in propylene oxide and embedded in Epon 812 resin (Electron Microscopy Sciences, Inc., Hatfield PA) and polymerized at 60 °C for 48 h. Sectioned on a Leica Ultracut R ultramicrotome (Leyca Microsystems, Wetzlar, DEU), and stained with 4% uranyl acetate and 0.3% Reynold lead citrate[49]. Micrographs were taken on a Jeol JEM-1010 (Jeol, Inc., JPN) electron microscope with an accelerating voltage of 80 kV and electron micrographs were captured with a CCD camera model Gatan Orius SC600 and a digital micrograph software.

Treatment of sporulating cells with the oxidizing agent H_2O_2. Strains were propagated in DSM under vigorous aeration (250 rpm) at 37 °C and their growth was monitored by optical density at 600 nm (OD_{600}). At 4.5 h after cessation of exponential growth ($t_{4.5}$), the culture was exposed to different doses of H_2O_2 in a concentration range of 0 to 75 mM for additional 1 h. The survival of sporulating cells during this treatment was measured by plating aliquots of serial dilutions in PBS on LB medium agar plates. The plates were grown overnight at 37 °C and the viable count was performed to determine the lethal doses 50 (LD_{50}) and 90 (LD_{90}).

Determination of spontaneous and H_2O_2-induced mutation frequencies in sporulating cells. Spontaneous and hydrogen peroxide induced Rif^R mutagenesis was performed according to a previously described protocol[13]. Briefly, strains were induced to sporulate at 37 °C in DSM. 4.5 h after t_0 (the time when the exponential and stationary phase slots intersect), the cultures were equally divided in two subcultures. One of these subcultures was left untreated and the other was amended with a lethal dose fifty (LD_{50}) of H_2O_2. Mutation frequencies to Rif^r were determined by plating aliquots of cells on six LB plates containing 10 mg/ml of rifampicin. Colonies resistant to rifampicin were counted after 24 h. The number of cells to calculate the mutation frequencies were obtained from aliquots of appropriate dilutions of the cultures plated on solid LB medium lacking rifampicin that were incubated for 24 h at 37 °C. The experiment was repeated at least three times.

Fluorescence microscopy. Fluorescence microscopy analysis of cells during sporulation was determined as previously described[9,13,34]. Briefly, *B. subtilis* strains wild-type and ΔGO Δ*mfd* were propagated in DSM at 37 °C. Cellular samples of both cultures were collected during 2, 5 and 9 h after t_0, corresponding to sporulation stages t_2, t_5 and t_9, respectively. Cell samples collected at the appropriate times were fixed, stained with DAPI and FM4-64 as previously described[34] and analyzed by epifluorescence microscopy employing a Zeiss Axioscope A1 microscope equipped with an AxioCam ICc1 camera. Fluorescence and bright field images were acquired by using AxioVision V 4.8.2 software and adjusted only for brightness and contrast as previously described[9,13,34]. Conditions employed for excitation and emission wavelengths were 350 and 470 nm for DAPI and 506 and 750 nm for FM4-64, respectively[9,13,34].

Confocal microscopy. Cell morphology during growth and sporulation was analyzed by phase contrast using confocal microscopy. *B. subtilis* cells were grown and induced to sporulate in DSM. Cellular samples of the wild-type strain, ΔGO Δ*mfd*, ΔGO and Δ*mfd* mutants were collected at the appropriate times, washed twice with cold phosphate-buffered saline [PBS; 0.7% Na2HPO4, 0.3% KH2PO4, 0.4% NaCl (pH 7.5)] and were fixed as described previously[20]. Phase contrast microscopy was performed with a Zeiss LSM700 scanning laser confocal microscope with a LD A-Plan 40x/0.55 Ph2 objective. Images were acquired and adjusted only for brightness and contrast with image software (Zen 2011, Carl Zeiss MicroImaging GHBH, Jena, Germany).

Statistical methods. For determination of sporulation frequency, lethal doses 90 (LD_{90}) and mutagenesis rate differences were calculated by performing one-way Analysis of Variance (ANOVA) followed by a Tukey's post-hoc analysis. Significance was set a $P < 0.05$. Analyses were performed with the OriginPro 2017.

Received: 16 October 2020; Accepted: 18 January 2021
Published online: 28 January 2021

References

1. Piggot, P. J. & Hilbert, D. W. Sporulation of *Bacillus subtilis*. *Curr. Opin. Microbiol.* **7**, 579–586 (2004).
2. Pedraza-Reyes, M., Ramírez-Ramírez, N., Vidales-Rodríguez, L. E. & Robleto, E. A. Mechanisms of bacterial spore survival.
3. Errington, J. Regulation of endospore formation in *Bacillus subtilis*. *Nat. Rev. Microbiol.* **1**, 117–126 (2003).

4. Fujita, M. & Losick, R. Evidence that entry into sporulation in *Bacillus subtilis* is governed by a gradual increase in the level and activity of the master regulator Spo0A. *Genes Dev.* **19**, 2236–2244 (2005).
5. Miller, A. K., Brown, E. E., Mercado, B. T. & Herman, J. K. A DNA-binding protein defines the precise region of chromosome capture during Bacillus sporulation: DNA-binding protein. *Mol. Microbiol.* **99**, 111–122 (2016).
6. Ruvolo, M. V., Mach, K. E. & Burkholder, W. F. Proteolysis of the replication checkpoint protein Sda is necessary for the efficient initiation of sporulation after transient replication stress in *Bacillus subtilis*. *Mol. Microbiol.* **60**, 1490–1508 (2006).
7. Bejerano-Sagie, M. *et al.* A checkpoint protein that scans the chromosome for damage at the start of sporulation in *Bacillus subtilis*. *Cell* **125**, 679–690 (2006).
8. Wagner, J. K., Marquis, K. A. & Rudner, D. Z. SirA enforces diploidy by inhibiting the replication initiator DnaA during spore formation in *Bacillus subtilis*. *Mol. Microbiol.* **73**, 963–974 (2009).
9. Ramírez-Guadiana, F. H., Barajas-Ornelas, R. D. C., Corona-Bautista, S. U., Setlow, P. & Pedraza-Reyes, M. The RecA-dependent SOS response is active and required for processing of DNA damage during *Bacillus subtilis* sporulation. *PLoS ONE*. https://doi.org/10.1371/journal.pone.0150348 (2016).
10. Rivas-Castillo, A. M., Yasbin, R. E., Robleto, E., Nicholson, W. L. & Pedraza-Reyes, M. Role of the Y-family DNA polymerases YqjH and YqjW in protecting sporulating *Bacillus subtilis* cells from DNA damage. *Curr. Microbiol.* **60**, 263–267 (2010).
11. Ramírez-Guadiana, F. H. *et al.* Alternative excision repair of ultraviolet B- and C-induced DNA damage in dormant and developing spores of *Bacillus subtilis*. *J. Bacteriol.* **194**, 6096–6104 (2012).
12. Setlow, B. & Setlow, P. Role of DNA repair in *Bacillus subtilis* spore resistance. *J. Bacteriol.* **178**, 3486–3495 (1996).
13. Ramírez-Guadiana, F. H. *et al.* Transcriptional coupling of DNA repair in sporulating *Bacillus subtilis* cells: Role of Mfd during *B. subtilis* sporulation. *Mol. Microbiol.* **90**, 1088–1099 (2013).
14. Ayora, S., Rojo, F., Ogasawara, N., Nakai, S. & Alonso, J. C. The Mfd protein of *Bacillus subtilis* 168 is involved in both transcription-coupled DNA repair and DNA recombination. *J. Mol. Biol.* **256**, 301–318 (1996).
15. Bidnenko, V. *et al.* Bacillus subtilis serine/threonine protein kinase YabT is involved in spore development via phosphorylation of a bacterial recombinase: *Bacillus subtilis* kinase YabT phosphorylates RecA. *Mol. Microbiol.* **88**, 921–935 (2013).
16. Ireton, K. & Grossman, A. D. A developmental checkpoint couples the initiation of sporulation to DNA replication in *Bacillus subtilis*. *EMBO J.* **13**, 1566–1573 (1994).
17. Lenhart, J. S., Schroeder, J. W., Walsh, B. W. & Simmons, L. A. DNA repair and genome maintenance in *Bacillus subtilis*. *Microbiol. Mol. Biol. Rev.* **76**, 530–564 (2012).
18. Brugger, C. *et al.* Molecular determinants for dsDNA translocation by the transcription-repair coupling and evolvability factor Mfd. *Nat. Commun.* **11**, 3740 (2020).
19. Hanawalt, P. C. & Spivak, G. Transcription-coupled DNA repair: Two decades of progress and surprises. *Nat. Rev. Mol. Cell Biol.* **9**, 958–970 (2008).
20. Valenzuela-García, L. I., Ayala-García, V. M., Regalado-García, A. G., Setlow, P. & Pedraza-Reyes, M. Transcriptional coupling (Mfd) and DNA damage scanning (DisA) coordinate excision repair events for efficient *Bacillus subtilis* spore outgrowth. *Microbiol. Open*. https://doi.org/10.1002/mbo3.593 (2018).
21. Vidales, L. E., Cárdenas, L. C., Robleto, E., Yasbin, R. E. & Pedraza-Reyes, M. Defects in the error prevention oxidized guanine system potentiate stationary-phase mutagenesis in *Bacillus subtilis*. *J. Bacteriol.* **191**, 506–513 (2009).
22. Michaels, M. L. & Miller, J. H. The GO system protects organisms from the mutagenic effect of the spontaneous lesion 8-hydroxyguanine (7,8-dihydro-8-oxoguanine). *J. Bacteriol.* **174**, 6321–6325 (1992).
23. Fromme, J. C. & Verdine, G. L. Structural insights into lesion recognition and repair by the bacterial 8-oxoguanine DNA glycosylase MutM. *Nat. Struct. Biol.* **9**, 544–552 (2002).
24. Banda, D. M., Nuñez, N. N., Burnside, M. A., Bradshaw, K. M. & David, S. S. Repair of 8-oxoG: A mismatches by the MUTYH glycosylase: Mechanism, metals and medicine. *Free Radic. Biol. Med.* **107**, 202–215 (2017).
25. Ramírez, M. I., Castellanos-Juárez, F. X., Yasbin, R. E. & Pedraza-Reyes, M. The ytkD (mutTA) gene of *Bacillus subtilis* encodes a functional antimutator 8-Oxo-(dGTP/GTP)ase and is under dual control of sigma A and sigma F RNA polymerases. *J. Bacteriol.* **186**, 1050–1059 (2004).
26. Castellanos-Juárez, F. X. *et al.* YtkD and MutT protect vegetative cells but not spores of *Bacillus subtilis* from oxidative stress. *J. Bacteriol.* **188**, 2285–2289 (2006).
27. Ross, C. *et al.* Novel role of mfd: effects on stationary-phase mutagenesis in *Bacillus subtilis*. *J. Bacteriol.* **188**, 7512–7520 (2006).
28. Gómez-Marroquín, M. *et al.* Stationary-phase Mutagenesis in stressed *Bacillus subtilis* cells operates by mfd-dependent mutagenic pathways. *Genes (Basel)* **7**, 33 (2016).
29. Leyva-Sánchez, H. C. *et al.* Role of mfd and GreA in *Bacillus subtilis* base excision repair-dependent stationary-phase mutagenesis. *J. Bacteriol.* https://doi.org/10.1128/JB.00807-19 (2020).
30. Barák, I. & Muchová, K. The positioning of the asymmetric septum during sporulation in *Bacillus subtilis*. *PLoS ONE* https://doi.org/10.1371/journal.pone.0201979 (2018).
31. Stragier, P. & Losick, R. Molecular genetics of sporulation in *Bacillus subtilis*. *Annu. Rev. Genet.* **30**, 297 (1996).
32. Higgins, D. & Dworkin, J. Recent progress in *Bacillus subtilis* sporulation. *FEMS Microbiol. Rev.* **36**, 131–148 (2012).
33. Fujita, M., González-Pastor, J. E. & Losick, R. High- and low-threshold genes in the Spo0A regulon of *Bacillus subtilis*. *J. Bacteriol.* **187**, 1357–1368 (2005).
34. Campos, S. S. *et al.* Interaction of apurinic/apyrimidinic endonucleases Nfo and ExoA with the DNA integrity scanning protein DisA in the processing of oxidative DNA damage during *Bacillus subtilis* spore outgrowth. *J. Bacteriol.* **196**, 568–578 (2014).
35. Rahn-Lee, L., Merrikh, H., Grossman, A. D. & Losick, R. The sporulation protein SirA inhibits the binding of DnaA to the origin of replication by contacting a patch of clustered amino acids. *J. Bacteriol.* **193**, 1302–1307 (2011).
36. Rowland, S. L. *et al.* Structure and mechanism of action of Sda, an inhibitor of the histidine kinases that regulate initiation of sporulation in *Bacillus subtilis*. *Mol. Cell* **13**, 689–701 (2004).
37. Martin, H. A. *et al.* Mfd protects against oxidative stress in *Bacillus subtilis* independently of its canonical function in DNA repair. *BMC Microbiol.* **19**, 26 (2019).
38. Zalieckas, J. M., Wray, L. V. Jr., Ferson, A. E. & Fisher, S. H. Transcription-repair coupling factor is involved in carbon catabolite repression of the *Bacillus subtilis* hut and gnt operons. *Mol. Microbiol.* **27**, 1031–1038 (1998).
39. Martin, H. A. *et al.* Mfd affects global transcription and the physiology of stressed *Bacillus subtilis* cells. *BioRxiv.* https://doi.org/10.1101/2020.11.27.401687 (2020).
40. Robleto, E. A. Mfd and transcriptional derepression cause genetic diversity in *Bacillus subtilis*. *Front. Biosci. (Elite Ed.)* **E4**, 1246–1254 (2012).
41. Burkholder, W. F., Kurtser, I. & Grossman, A. D. Replication initiation proteins regulate a developmental checkpoint in *Bacillus subtilis*. *Cell* **104**, 269–279 (2001).
42. Veening, J.-W., Murray, H. & Errington, J. A mechanism for cell cycle regulation of sporulation initiation in *Bacillus subtilis*. *Genes Dev.* **23**, 1959–1970 (2009).
43. Brégeon, D., Doddridge, Z. A., You, H. J., Weiss, B. & Doetsch, P. W. Transcriptional mutagenesis induced by uracil and 8-oxoguanine in *Escherichia coli*. *Mol. Cell* **12**, 959–970 (2003).
44. Witte, G., Hartung, S., Büttner, K. & Hopfner, K.-P. Structural biochemistry of a bacterial checkpoint protein reveals diadenylate cyclase activity regulated by DNA recombination intermediates. *Mol. Cell* **30**, 167–178 (2008).

45. Sambrook, J., Fritsch, E. F. & Maniatis, T. *Molecular Cloning: A Laboratory Manual* (Cold Spring Harbor Laboratory, Cold Spring Harbor, 1989).
46. Miller, J. H. *Experiments in Molecular Genetics* (Cold Spring Harbor Laboratory, Cold Spring Harbor, 1972).
47. Schaeffer, P., Millet, J. & Aubert, J. P. Catabolic repression of bacterial sporulation. *Proc. Natl. Acad. Sci. U.S.A.* **54**, 704–711 (1965).
48. Harwood, C. R. & Cutting, S. M. *Molecular Biological Methods for Bacillus* (Wiley, Hoboken, 1990).
49. del Barajas-Ornelas, R. C. *et al.* Error-prone processing of apurinic/apyrimidinic (AP) sites by PolX underlies a novel mechanism that promotes adaptive mutagenesis in *Bacillus subtilis*. *J. Bacteriol.* **196**, 3012–3022 (2014).
50. Nicholson, W. L. & Setlow, P. Sporulation, germination and outgrowth. In *Molecular Biological Methods for Bacillus* (eds Harwood, C. R. & Cutting, S. M.) 391–450 (Wiley, Chichester, 1990).
51. Santo, L. Y. & Doi, R. H. Ultrastructural analysis during germination and outgrowth of *Bacillus subtilis* spores. *J. Bacteriol.* **120**, 475–481 (1974).

Acknowledgements

This work was supported by the National Council of Science and Technology (CONACYT; Grants 221231 and A1-S-27116) of México and the University of Guanajuato (Grants CIIC 228/2019 and CIIC 178/2020). This work was also funded by the NIH (GM131410). V.P. S, L.E. M, and H.C. L-S were supported by scholarships from CONACyT.

Author contributions

M.P.-R. designed the study and wrote the manuscript. E.A.R., H.C.L.-S., M.C.-C. and L.F.J.-G., wrote the manuscript. V.P.S., L.E.M., N.R.-R., A.O.-H., R.L.-M., L.I.V.-G. and H.C.L.-S., carried out the genetic and microscopy analyses.

Competing interests

The authors declare no competing interests.

Additional information

Supplementary Information The online version contains supplementary material available at https://doi.org/10.1038/s41598-021-82247-8.

Correspondence and requests for materials should be addressed to M.P.-R.

Reprints and permissions information is available at www.nature.com/reprints.

Publisher's note Springer Nature remains neutral with regard to jurisdictional claims in published maps and institutional affiliations.